Mineralogical Magazine, August 2012, Vol. 76(4), pp. 839–849

Refinement of the crystal structure of zoned philipsbornite–hidalgoite from the Tsumeb mine, Namibia, and hydrogen bonding in the $D^{2+}G_3^{3+}(T^{5+}O_4)(TO_3OH)(OH)_6$ alunite structures

M. A. Cooper and F. C. Hawthorne*

Department of Geological Sciences, University of Manitoba, Winnipeg, Manitoba R3T 2N2, Canada

[*Received 19 January 2012; Accepted 19 March 2012; Associate Editor: G. Diego Gatta*]

ABSTRACT

The crystal structure of zoned philipsbornite–hidalgoite, hexagonal (rhombohedral), $R\bar{3}m$, $Z = 3$: $a = 7.1142(4)$, $c = 17.0973(9)$ Å, $V = 749.4(1)$ Å^3, from the Tsumeb mine, Namibia, has been refined to $R_1 = 1.68\%$ for 301 unique reflections collected on a Bruker D8 three-circle diffractometer equipped with a rotating-anode generator, multilayer optics and an APEX-II CCD detector. Chemical analysis by electron microprobe showed zoned crystals with a rim enriched in S and Fe relative to the core. The core composition is SO_3 3.31, As_2O_5 30.57, Al_2O_3 23.05, FeO 1.44, PbO 33.94, H_2O_{calc} 9.58, total 101.79 wt.%, corresponding to $Pb^{2+}_{0.98}(Al_{2.92}Fe^{2+}_{0.13})(AsO_4)[(As_{0.72}S_{0.27})O_{3.14}(OH)_{0.85}](OH)_6$; and the rim composition is SO_3 8.88, As_2O_5 22.63, Al_2O_3 22.90, FeO 2.57, PbO 34.91, H_2O_{calc} 9.27, total 101.16 wt.%, corresponding to $Pb^{2+}_{0.99}(Al_{2.85}Fe^{2+}_{0.23})(AsO_4)[(As_{0.25}S_{0.70})O_{3.30}(OH)_{0.50}](OH)_6$. Philipsbornite–hidalgoite has the alunite-type structure, sheets of corner-sharing octahedra, decorated on top and bottom by $[(As,S)O_4]$ and (AsO_3OH) tetrahedra, that are linked into a three-dimensional structure by [12]-coordinated Pb^{2+} cations and hydrogen bonds. A new hydrogen-bonding scheme for the $D^{2+}G_3^{3+}(T^{5+}O_4)(TO_3OH)(OH)_6$ minerals is proposed.

Keywords: philipsbornite, hidalgoite, crystal structure, arsenate, alunite supergroup, electron-microprobe analysis, hydrogen bonding.

Introduction

Philipsbornite, ideally $Pb^{2+}Al_3(AsO_4)(AsO_3OH)(OH)_6$, is an arsenate mineral first described by Walenta *et al.* (1982) from Dundas, Tasmania. Hidalgoite, ideally $Pb^{2+}Al_3(As_{0.5}S_{0.5}O_4)_2(OH)_6$, is a mixed arsenate-sulfate mineral first described by Smith *et al.* (1953) from the San Pascual mine, Hidalgo, Mexico. Schmetzer *et al.* (1982) reported the occurrence of philipsbornite from the Tsumeb mine, Tsumeb, Namibia, and Gebhard (1999) reported the occurrence of hidalgoite from the Tsumeb mine. Philipsbornite and hidalgoite are members of the alunite supergroup which Bayliss *et al.* (2010) write as $DG_3(TO_4)_2X'_6$ where D = monovalent (e.g. K, Na, NH_4, H_3O), divalent (e.g. Ca, Ba, Pb^{2+}) and trivalent (e.g. Bi, *REE*) cations; G = dominantly trivalent (Al, Fe^{3+}) but also quadrivalent (Sn^{4+}) and divalent (Cu^{2+}, Zn, Mg) cations; T = hexavalent (e.g. S^{6+}, Cr^{6+}), pentavalent (e.g. P, As^{5+}) and quadrivalent (Si) cations; X′ = O, (OH), F, (H_2O). Philipsbornite belongs to the dussertite group and hidalgoite belongs to the beudantite group (both with 1*c*). Many years ago, we were asked by William W. Pinch to identify some extremely small white hexagonal tablets from the Tsumeb mine, Namibia (Weber and Wilson, 1977; Pinch and

* E-mail: frank_hawthorne@umanitoba.ca
DOI: 10.1180/minmag.2012.076.4.02

Wilson, 1977), but these proved too small to obtain any signal from single-crystal diffraction. Recent acquisition of a more powerful radiation source provided us with a single-crystal diffraction pattern that indicated these crystals to be a member of the alunite supergroup. Electron-microprobe analysis showed the mineral to be zoned from philipsbornite in the core to hidalgoite in the rim, and we present a refinement of the crystal structure here.

X-ray data collection and structure-refinement

X-ray-diffraction data were collected with Mo$K\alpha$ radiation on a Bruker D8 three-circle diffractometer equipped with a rotating-anode generator, multilayer optics and an APEX-II CCD detector. The intensities of 8723 reflections (2874 in the Ewald sphere) were collected to 60º 2θ using 5 s per 0.3º frame with a crystal-to-detector distance of 5 cm. An empirical absorption correction (*SADABS*; Sheldrick, 2008) was applied, and the data were corrected for Lorentz, polarization and background effects. The refined unit-cell parameters (Table 1) were obtained from 7465 reflections with $I > 10\sigma I$. The structure was refined in the space groups $R\bar{3}m$ and $R3m$ with the *SHELXTL* version 5.1 system of programs (Bruker, 1997). The final models refined to R_1 indices of 1.68% ($R\bar{3}m$, 301 reflections, 33 variable parameters) and 1.61% ($R3m$, 593 reflections, 56 variable parameters). The refined parameters are the same within their respective assigned standard deviations for both space groups.

The Pb^{2+} cation at the *Pb* site shows a larger displacement in the **a-b** plane than along **c** and was allowed to refine off the 3-fold axis. Previous work has used several different models for this displacement. Giuseppettii and Tadini (1980, 1987) placed Pb at (0, 0, 0) (the 3*a* site) in osarizawaite and corkite (but with large displacement parameters), Szymanski (1985) used this model for plumbojarosite, and Sato *et al.* (2009) also used this model for corkite. Grey *et al.* (2009) placed Pb at (x, 0, 0) (the 18*f* site) in kintoreite and zinc-bearing kintoreite, and our results are in accord with this model. The H site associated with the (OH) group of the $Al(OH)_4O_2$ octahedron was identified in the difference-Fourier map and inserted into the refinement with the soft constraint that the O_D–H distance remain close to 0.98 Å. Details of the data collection and structure refinement are given in Table 1, final atom parameters are given in Table 2, selected interatomic distances and angles in Table 3, refined site-scattering values (Hawthorne *et al.*, 1995) and site populations in Table 4, and bond valences in Table 5. A table of structure factors has been deposited with the Principal Editor of *Mineralogical Magazine* and is available from www.minersoc.org/pages/e_journals/dep_mat.html.

Chemical composition

The crystal used for chemical analysis was not the crystal used in the collection of the X-ray intensity data as we wished to preserve the latter. The crystal was mounted in epoxy, polished, and analysed using a Cameca SX-100

TABLE 1. Crystallographic data and structure-refinement information for philipsbornite–hidalgoite.

a (Å)	7.1142(4)	Crystal size (μm)	$7 \times 80 \times 100$
c (Å)	17.0973(9)	Radiation/filter	Mo$K\alpha$/graphite
V (Å^3)	749.39(12)	Total reflections	8723
Space group	$R\bar{3}m$	No. in Ewald sphere	2874
Z	3	No. unique reflections	301
		$\|F_o\| > 4\sigma F$	301
		R_{merge} (%)	2.07
		R_1 (%)	1.68
		wR_2 (%)	4.31
		GooF	1.323

$R_1 = \Sigma(|F_o| - |F_c|)/\Sigma|F_o|$
$wR_2 = \{\Sigma[w(F_o^2 - F_c^2)^2] / \Sigma[w(F_o^2)^2]\}^{½}$
$w = 1 / [\sigma^2(F_o^2) + (0.0141P)^2 + 6.07P]$, where $P = (F_o^2 + 2F_c^2) / 3$

TABLE 2. Atom coordinates and displacement parameters for phillipsbornite–hidalgoite.

Atom	*x/a*	*y/a*	*z/c*	U_{eq}	U_{11}	U_{22}	U_{33}	U_{23}	U_{13}	U_{12}
Pb	0.027(4)	0	0	0.025(4)	0.028(3)	0.029(11)	0.0173(2)	−0.0015(14)	−0.0007(7)	0.014(6)
Al	½	0	½	0.0088(4)	0.0091(5)	0.0065(6)	0.0099(6)	0.0003(4)	0.0001(2)	0.0033(3)
As	0	0	0.30936(4)	0.0098(2)	0.0087(3)	0.0087(3)	0.0119(4)	0	0	0.00433(12)
O(1)	0	0	0.5943(3)	0.0185(9)	0.0177(13)	0.0177(13)	0.020(2)	0	0	0.0089(7)
O(2)	0.2073(2)	0.7927(2)	−0.05806(14)	0.0131(5)	0.0155(8)	0.0155(8)	0.0108(9)	0.0004(4)	−0.0004(4)	0.0097(9)
O(3)	0.12428(19)	0.87572(19)	0.14032(14)	0.0102(4)	0.0083(7)	0.0083(7)	0.0136(10)	−0.0011(4)	0.0011(4)	0.0038(8)
H(1)	0.1970(18)	0.8030(18)	0.117(3)	0.031(14)						

electron microprobe. Preliminary analysis was done using energy-dispersive spectrometry (EDS) to assess the major-element composition of the crystal. Following this, elements were quantitatively analysed in wavelength-dispersive mode using an accelerating voltage of 15 kV, a beam current of 10 nA and a beam size of 5 μm. The following standards were used for *K*α lines: Pb, synthetic PbTe; As, cobaltite; Al, andalusite; S, pyrite; Fe, fayalite. The elements K, Na, Tl, Ca, Ba, Sr, Cd, Mg, V, Cr, Mn, Ni, Cu, Zn, Ga, Si, Ge and P were sought but not detected. Data were corrected using the PAP procedure of Pouchou and Pichoir (1985). The crystal was strongly zoned with a distinct core and rim of significantly different compositions (Table 6). Exposure to the vacuum resulted in cracking of the crystal.

Calculation of the chemical formula

The crystal used for the electron-microprobe analysis is a solid solution between philipsbornite, ideally $Pb^{2+}Al_3(AsO_4)(AsO_3OH)(OH)_6$, and hidalgoite, ideally $Pb^{2+}Al_3(As_{0.5}S_{0.5}O_4)_2(OH)_6$ which we will write here as $Pb^{2+}Al_3(AsO_4)(SO_4)(OH)_6$ without implying that As and S occupy crystallographically distinct sites. In a solid solution between these two minerals, the (OH) content varies from 6 to 7 a.p.f.u., somewhat complicating the calculation of the chemical formula. Starting from the endmember formula of philipsbornite, (OH) may be replaced by O^{2-} in the acid arsenate group via the substitution $(SO_4)^{2-} \rightarrow (AsO_3OH)^{2-}$ and Fe may enter the structure via the substitutions $(SO_4)^{2-} + Fe^{2+} \rightarrow (AsO_4)^{3-} + Al$ and $Fe^{3+} \rightarrow Al$. As S > Fe in the crystals analysed, the substitution $Fe^{3+} \rightarrow Al$ is negligible and we will ignore it here. We may write an interim general formula for our crystal as follows: $Pb^{2+}Al_{(3-a-b)}(SO_4)_{(a+b)}Fe^{2+}_a(AsO_4)_{(1-a)}(AsO_3OH)_{(1-b)}(OH)_6$, where the (OH) content is $(7 - b)$ a.p.f.u. From the chemical analysis, we may derive $Al = (3 - a - b)$, $Fe = a$, and $S = (a + b)$, from which we may determine a and b. This in turn allows us to estimate the (OH) content and we may recalculate the formula using this value; this process may be iterated to convergence. The chemical formulae corresponding to the compositions with the maximum and minimum contents of S are given in Table 6, calculated on the basis of $OH = (7 - b)$ a.p.f.u. (where b is the amount of S minus the amount of Fe). As is apparent from Table 6, the core of the crystal is philipsbornite and the rim of the crystal is hidalgoite.

TABLE 3. Selected interatomic distances (Å) and angles in philipsbornite–hidalgoite.

As–O(1)	1.647(5)		*Pb*–O(2)	2.59(2) ×2
As–O(3)	1.659(3)	×3	*Pb*–O(2)′	2.747(3) ×2
<*As*–O>	1.656		*Pb*–O(2)″	2.90(2) ×2
			Pb–O(3)	2.763(12) ×2
Al–O(2)	1.923(2)	×2	*Pb*–O(3)′	2.853(3) ×2
Al–O(3)	1.9028(8)	×4	*Pb*–O(3)″	2.940(15) ×2
<*Al*–O>	1.910		<*Pb*–O>	2.799
O(3)–H(1)	0.98		O(3)–O(1)	2.826(3)
			O(3)–O(2)	3.543(3)
H(1)···O(1)	1.846(3)			
H(1)···O(2)	3.00(5)		O(3)–H(1)···O(1)	179(5)
			O(3)–H(1)···O(2)	116(4)

Description of the structure

The alunite structure has been described extensively elsewhere (e.g. Kolitsch and Pring, 2001; Kolitsch *et al.*, 1999*a*,*b*; Dzikowski *et al.*, 2006; Sato *et al.*, 2009; Mills *et al.*, 2009). The structure consists of layers of corner-sharing octahedra that are decorated top and bottom by tetrahedra that link by sharing three apices with the octahedra (Fig. 1). The remaining apex, the O(1) anion, is either an O atom in an $(AsO_4)^{3-}$ group or is an (OH) anion in an acid-arsenate group: $(AsO_3(OH))^{2-}$. The layers are held together by Pb^{2+} cations that are [12]-coordinated.

Site populations were assigned on the basis of the refined site-scattering factors (Table 4), and lie between the maximum and minimum values of S given by the chemical compositions listed in Table 6. The calculated content of Fe lies outside the limits given in Table 6 (for a different crystal), but is still significantly less that the amount of S indicated by the refined site-scattering values.

The (TO_4)–(TO_3OH)–$(OH)_6$ component

For the $D^{2+}G_3^{3+}(T^{5+}O_4)(T^{5+}O_3OH)(OH)_6$ minerals (Table 7), the tetrahedrally coordinated component of the structure consists ideally of equal amounts of $(T^{5+}O_4)$ and $(T^{5+}O_3OH)$. The structures are generally refined in the space group $R\bar{3}m$, with three crystallographically distinct anions: O(1) = $[O^{2-}, (OH)]_2$; O(2) = O_6^{2-}; O(3) = $(OH)_6$, to give 14 anions per formula unit. Two $(T^{5+}\Phi_4)$ [Φ = unspecified anion] tetrahedra occur along the 3-fold axis with opposing O(1) apices, as shown schematically in Fig. 2. The general consensus has been that the (OH) group at O(3) forms a hydrogen bond with the O(1) anion, each O(1) anion receiving a total of three such hydrogen bonds. One half of the O(1) anions are occupied by (OH) groups, with the hydrogen bond directed toward the adjacent O(1) anion (i.e. O^{2-}) of the opposing $(T^{5+}O_4)$ group. In Fig. 2, we have assigned representative bond valences (using the curves of Brown and Altermatt, 1985) to a local $(T^{5+}O_4)$–$(T^{5+}O_3OH)$

TABLE 4. Refined site-scattering values and site populations in philipsbornite–hidalgoite.

Site	Refined site-scattering (e.p.f.u.)	Site-population (a.p.f.u.)	Range in EMP composition (a.p.f.u.)
Pb	82	Pb^{2+}	$Pb^{2+}_{0.98-0.99}$
Al	44.1(3)	$Al_{2.562}$ $Fe_{0.438}$	$Al_{2.87-2.77}$ $Fe_{0.13-0.23}$
As	59.2(3)	$As_{0.824}$ $S_{0.176}$	$As_{1.73-1.30}$ $S_{0.27-0.70}$

TABLE 5. Bond-valence (vu) table for philipsbornite–hidalgoite.

	Pb	*Al*	*As*	Σ
O(1)			1.38	1.38
O(2)	0.27 $^{\times 2}\downarrow$	0.48 $^{\times 2}\downarrow$	1.34 $^{\times 3}\downarrow$	1.94→2.09
	0.18 $^{\times 2}\downarrow$			
	0.12 $^{\times 2}\downarrow$			
O(3)	0.17 $^{\times 2}\downarrow$	0.51 $^{\times 2}\rightarrow{}^{\times 4}\downarrow$		1.13–1.19
	0.13 $^{\times 2}\downarrow$			
	0.11 $^{\times 2}\downarrow$			
Σ	1.96	3.00	5.40	

* bond-valence parameters (vu) from Brown and Altermatt (1985).

configuration. In order to obtain the most representative bond valences for the T–O(1) and T–O(2) interactions, we averaged the values for the five structures in Table 7 in which the bond-valence sum at the *T* site is in close agreement with the valence-sum rule (i.e. 4.96–5.01 vu, for crandallite, goyazite, kintoreite, Ga-rich plumbogummite and dussertite); this gives a mean value of 1.29 vu for the T–O(1) bond and 1.23 vu for the T–O(2) bond. The chemical data associated with these five structure refinements also indicate near endmember *T*-site compositions.

The O(3)–O(1) distances and O(3)–H(1)···O(1) angles are typical hydrogen-bond geometries with corresponding H(1)···O_A bond valences of approximately 0.2 vu. The longer O(1)–O(1) separation (≥3 Å) suggests a weaker H(2)···$O(1)_A$ contribution (≤0.1 vu). The ensuing incident bond-valence sums at $O(1)_D$ [D = donor anion] and $O(1)_A$ [A = acceptor anion] are 2.79 and 1.99 vu, respectively. It is immediately apparent that the high bond valence incident at $O(1)_D$ (2.79 vu) indicates that there is a problem with a particular O(1) site being occupied by an (OH) group that also receives three hydrogen bonds from the neighbouring (OH) group at O(3). To help accord with the valence-sum rule at $O(1)_D$, the incident bond-valence sum could be partly reduced by

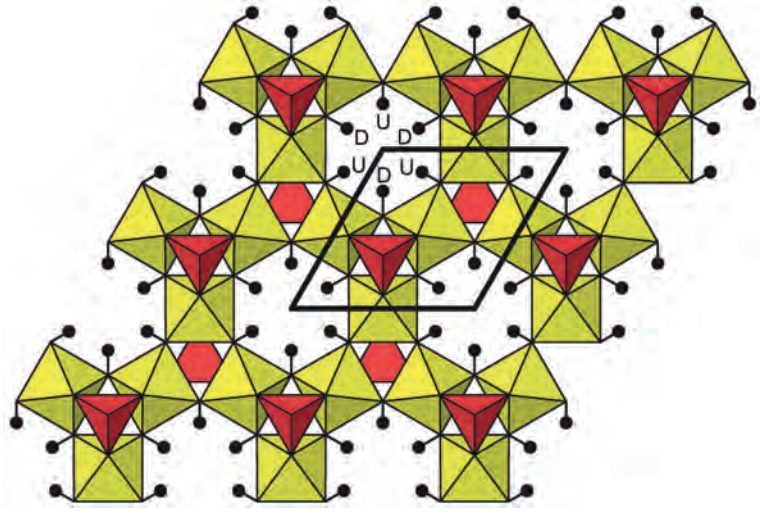

FIG. 1. One layer of the crystal structure of philipsbornite–hidalgoite viewed down *c*; the As tetrahedra are red; Al octahedra are yellow; H is represented by black circles; U, H pointing up; D, H pointing down; black lines are the outline of the unit cell.

TABLE 6. Chemical composition (wt.%) and formula (a.p.f.u.) for a zoned philipsbornite–hidalgoite crystal.

	Core	Rim
As_2O_5	30.57	22.63
SO_3	3.31	8.88
Al_2O_3	23.05	22.90
FeO	1.44	2.57
PbO	33.94	34.91
H_2O	9.58	9.27
Sum	101.79	101.16
As^{5+}	1.72	1.25
S^{6+}	0.27	0.70
Sum	1.99	1.95
Al	2.92	2.85
Fe^{2+}	0.13	0.23
Sum	3.05	3.08
Pb^{2+}	0.98	0.99
(OH)	6.86	6.53

Not detected: Ca, Ba, Sr, K, Na, Tl, Cd, Ga, Zn, Mg, Ni, Cu, Mn, Cr, P, V, Si, Ge.

lengthening the T–$O(1)_D$ bond (which needs to occur for 50% of the local arrangements). However, the displacement parameters for the *T* and O(1) sites do not suggest any significant positional disorder. We must conclude that where O(1) is occupied by an (OH) group, the locally associated $O(1)_D$ anion does not receive any hydrogen-bond contribution from the (OH) group at O(3); the resulting bond valence incident at $O(1)_D$ is then 1.29 + 0.90 = 2.19 vu, and the hydrogen bond from the adjacent (OH) group at O(3) must have another acceptor anion.

The optimum acceptor for this hydrogen bond is the O(2) anion at the base of the ($T^{5+}O_3OH$) tetrahedron. The O(2) anion is [3]-coordinated and forms bonds with each of the D, G and T cations. For the five $D^{2+}G_3^{3+}(T^{5+}O_4)(T^{5+}O_3OH)(OH)_6$ minerals in Table 7, the bond valences incident at the O(2) anion are given in Table 8. There is little variation in the G–O(2) and T–O(2) contributions, but the positional disorder associated with the D cation gives rise to different local arrangements involving (and different bond-valence contributions to) the O(2) anion. In goyazite and dussertite, where the D cation is reasonably well ordered, the bond

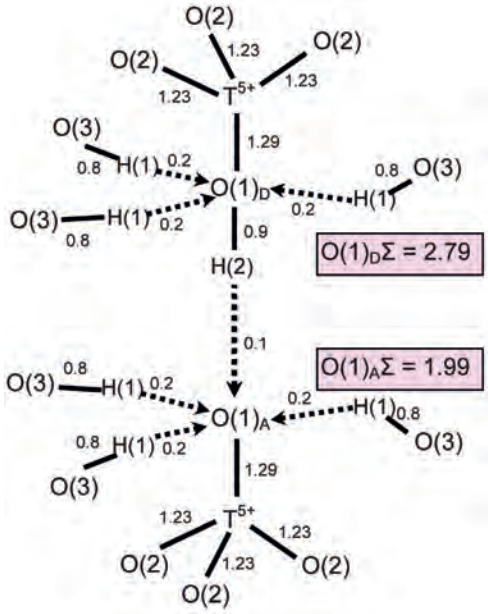

FIG. 2. General schematic showing representative bond-valence values (vu) associated with previously proposed hydrogen-bonding schemes for five $D^{2+}G_3^{3+}(T^{5+}O_4)(T^{5+}O_3OH)(OH)_6$ structures.

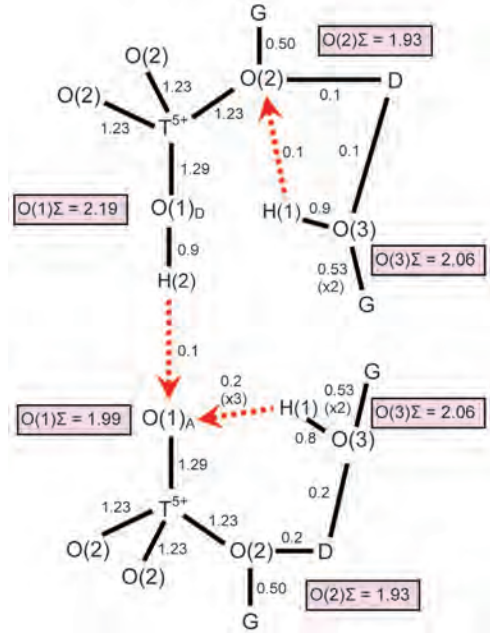

FIG. 3. Proposed hydrogen-bond arrangement and bond-valence distribution (vu) for the $D^{2+}G_3^{3+}(T^{5+}O_4)(T^{5+}O_3OH)(OH)_6$ structures.

TABLE 7. Selected minerals of the form $D^{2+}G_3^{3+}(T^{5+}O_4)(T^{5+}O_3OH)(OH)_6$ with space group $R\bar{3}m$.

	Crandallite	Goyazite	Kintoreite	Plumbogummite	Plumbogummite (Ga-rich)	Gorceixite	Dussertite	Springcreekite
D cation	Ca	Sr	Pb	Pb	$Pb_{0.88}Ca_{0.12}$	Ba	Ba	Ba
G cation	Al_3	Al_3	Fe_3	Al_3	$Al_{1.95}Ga_{1.05}$	Al_3	$Fe_{0.84}Sb_{0.16}$	$V_{0.57}Fe_{0.43}$
T cation	P_2	P_2	P_2	$P_{0.95}As_{0.05}$	P(S)*$_2$	P_2	As_2	P_2
a (Å)	7.005	7.015	7.296	7.039	7.075	7.054	7.410	7.243
c	16.192	16.558	16.849	16.761	16.818	17.275	17.848	17.3854
T–O(1) (Å)	1.520	1.536	1.512	1.537	1.507	1.563	1.689	1.554
T–O(2) ×3	1.543	1.535	1.545	1.561	1.542	1.538	1.683	1.540
<T–O>	1.537	1.535	1.537	1.555	1.533	1.544	1.685	1.544
T–O(1) (vu)	1.30	1.24	1.33	1.24	1.35	1.16	1.23	1.19
T–O(2) ×3	1.22	1.25	1.21	1.16	1.22	1.24	1.25	1.23
(T–O) Σ	4.96	4.99	4.96	4.72	5.01	4.88	4.98	4.88
O(1)–O(1) (Å)	2.992	3.302	3.215	3.295	3.411	3.738	3.249	3.672
O(3)–O(1)	2.729	2.788	2.801	2.781	2.811	2.884	2.879	2.891
O(3)–H(1)	–	0.95	0.90	–	0.90	0.98	–	–
O(3)–O(2)	3.239	3.388	3.312	3.440	3.421	3.622	3.592	3.533
H(1)···O(1)	–	1.84	1.96	–	1.92	1.90	–	–
H(1)···O(2)	–	2.77	2.59	–	2.88	2.99	–	–
O(3)–H(1)–O(1)°	–	175.6	157.1	–	179.1	179.4	–	–
O(3)–H(1)–O(2)°	–	123.1	137.2	–	120.1	123.5	–	–
D *x* coordinate	0.0440	0	0.0537	0.0409	0.033	0	0	0
D–O(2) ×2	2.461	2.767	2.590	2.554	2.614	2.825	2.863	2.902
D–O(2) ×2	2.757	2.767	2.931	2.797	2.817	2.825	2.863	2.902
D–O(2) ×2	3.025	2.767	3.237	2.919	3.007	2.825	2.863	2.902
D–O(3) ×2	2.506	2.729	2.574	2.644	2.647	2.859	2.885	2.842
D–O(3) ×2	2.678	2.729	2.778	2.785	2.766	2.859	2.885	2.842
D–O(3) ×2	2.839	2.729	2.968	3.022	2.880	2.859	2.885	2.842
References†	(1)	(2)	(3)	(4)	(5)	(6)	(7)	(8)

* 2–3 % S may be present (Mills *et al*. 2009).

† References: (1) Blount (1974); (2) Kato (1987); (3) Grey *et al.* (2009); (4) Kolitsch *et al.* (1999*c*); (5) Mills *et al.* (2009); (6) Dzikowski *et al.* (2006); (7) Kolitsch *et al.* (1999*a*); (8) Kolitsch *et al.* (1999*b*).

TABLE 8. Bond valence (vu) incident at the O(2) and O(3) anions in selected $D^{2+}G_3^{3+}(T^{5+}O_4)(T^{5+}O_3OH)(OH)_6$ minerals.

	Crandallite	Goyazite	Kintoreite	Plumbogummite Ga-rich	Dussertite
O(2)–D	0.06–0.26	0.17	0.05–0.27	0.09–0.25	0.21
O(2)–G	0.47	0.50	0.46	0.49	0.54
O(2)–T	1.22	1.25	1.21	1.22	1.25
O(2) Σ	1.75–1.95	1.92	1.72–1.94	1.80–1.96	2.00
O(3)–D	0.09–0.23	0.19	0.10–0.29	0.12–0.23	0.20
O(3)–G (×2)	0.53	0.53	0.53	0.53	0.57
O(3) Σ	1.15–1.29	1.25	1.16–1.35	1.18–1.29	1.34

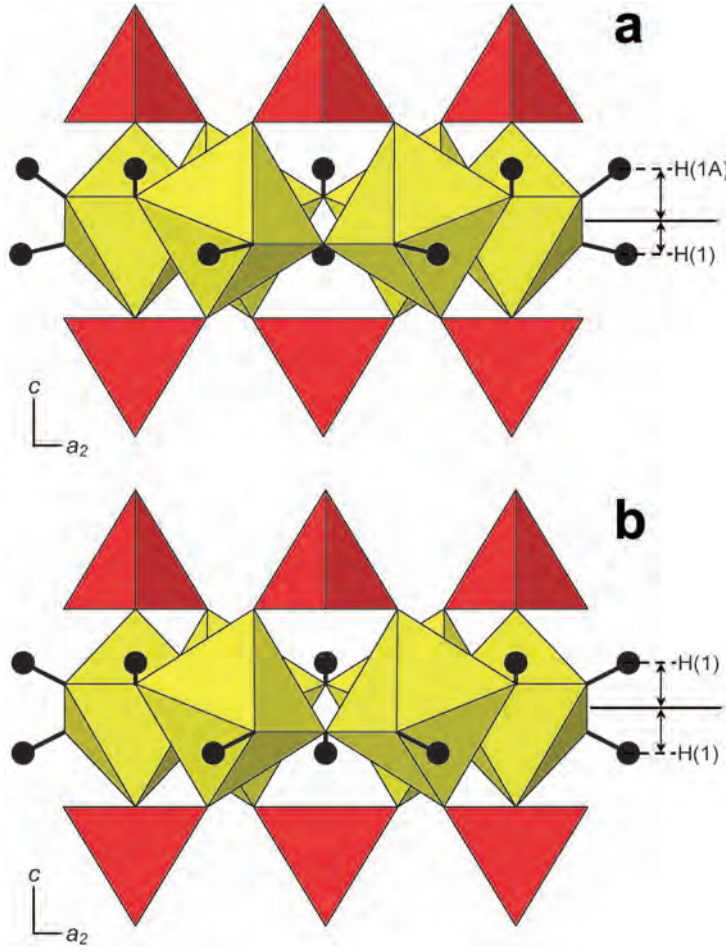

FIG. 4. The structure of philipsbornite–hidalgoite projected onto (100) showing (*a*) the difference in short-range H positions associated with the (OH) group of the $Al(OH)_4O_2$ octahedron, and (*b*) the ideal long-range positions of the H atoms. The As tetrahedra are red; Al octahedra are yellow and H is represented by black circles.

valences incident at O(2) are close to that required by the valence-sum rule (1.92 and 2.00 vu, respectively). In crandallite, kintoreite and Ga-rich plumbogummite, the sums range from deficient (~1.75 vu) to near ideal (~1.95 vu). It seems that positional disorder of the D cation can lead to slight deviation from the valence-sum rule at O(2), making O(2) a more favourable hydrogen-bond acceptor where this disorder occurs.

The O(3)–O(2) distances range from 3.239 to 3.622 Å (Table 7), indicating that the hydrogen-bond valence to O(2) from the (OH) group at O(3) will be small (i.e. $\leqslant$0.1 vu). We propose that the hydrogen-bonding scheme shown in Fig. 3 occurs in the $D^{2+}G_3^{3+}(T^{5+}O_4)(T^{5+}O_3OH)(OH)_6$ minerals of the alunite group. Where the $(T^{5+}\Phi_4)$ group contains an (OH) group at O(1), the neighbouring (OH) groups at O(3) have weak hydrogen bonds with the O(2) anions at the base of the $(T^{5+}\Phi_4)$ tetrahedron, and in this case, the D cation is further from the O(2) and O(3) anions; the resulting incident bond-valence sums at O(1), O(2) and O(3) are 2.19, 1.93 and 2.06 vu, respectively. The opposing $(T^{5+}\Phi_4)$ group receives a weak hydrogen bond at its $O(1)_A$ vertex and three additional hydrogen bonds from the peripheral (OH) groups at O(3), and the D cation is closer to the adjacent O(2) and O(3) anions; the incident bond-valence sums at O(1), O(2) and O(3) are 1.99, 1.93 and 2.06 vu, respectively. For goyazite and dussertite, in which positional disorder of the D cation was not reported, the same pattern of hydrogen bonding may occur, and the structure may respond in a slightly different manner. For example, where the D cation is disordered off the 3-fold axis, T–O(1) < T–O(2), and the D cation occurs on the 3-fold axis, T–O(1) > T–O(2) (Table 7). The relative apical lengthening (or flattening) of the $(T^{5+}\Phi_4)$ group seems to correlate with the positional order-disorder of the D cation.

The philipsbornite–hidalgoite solid solution: short-range aspects of hydrogen bonding

Within the central region of each six-membered ring of corner-sharing $Al(OH)_4O_2$ octahedra, three H atoms point upward and three point downward (Fig. 1). The long-range positions of the H atoms above and below the central axis of the ring of octahedra are the same in $R\bar{3}m$ symmetry (Fig. 4*b*), but may differ at short range (e.g. local $R3m$ symmetry, Fig. 4*a*). In Fig. 4*a*, the H atoms above and below the central axis of the ring differ appreciably in their geometric relation to the proposed hydrogen-bonding scheme (Fig. 5). The H(1) atom lies closer to the central axis of the ring (Fig. 4*a*) and is in a favourable position to form a hydrogen bond with the O(1A) anion (at the apex of the As(1A) tetrahedron) (Figs 5 and 6). The H(1A) atom lies further from the central axis of the ring (Fig. 4*a*) and is in a favourable position to form a weak hydrogen bond with the O(2) anion (at the base of the As(1) tetrahedron) (Figs 5 and 6). The hydrogen-bond arrangements involving H(1) and H(1A) combine with the inferred H(2) position (not located in the refinement) belonging to the (OH) group of the As(1) tetrahedron (Fig. 5) in

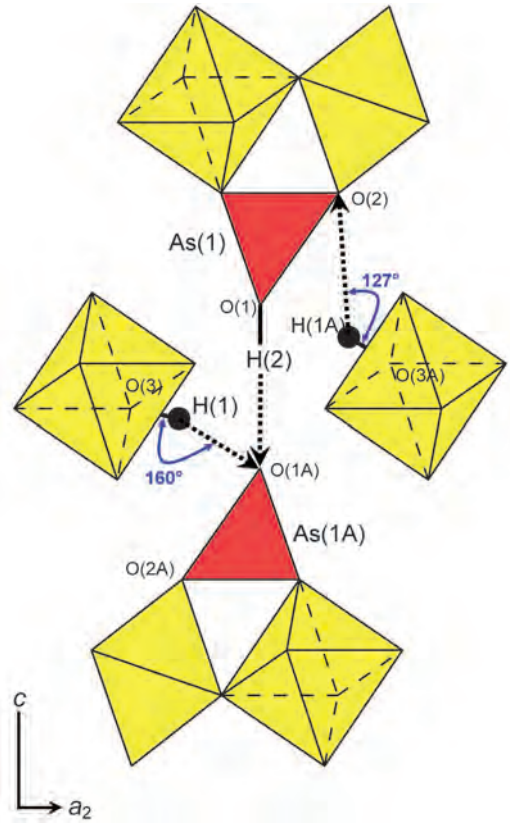

FIG. 5. The $R3m$ structure of philipsbornite–hidalgoite projected down [100], showing the proposed hydrogen-bond arrangement. The As tetrahedra are red; Al octahedra are yellow and H is represented by black circles.

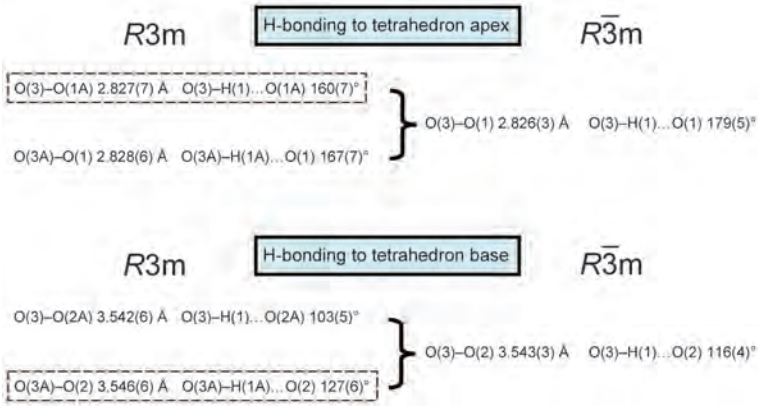

FIG. 6. The hydrogen-bond geometries for philipsbornite–hidalgoite. The short-range arrangements (locally in accord with *R3m* symmetry) enclosed in dashed outlines are the preferred arrangements.

the bond-valence arrangement of Table 5, where the sums are in close accord with the valence-sum rule (Brown, 2002). The complete hydrogen-bond arrangement in this crystal (Fig. 5; Table 5) supports the schematic presented in Fig. 3 for the $D^{2+}G_3^{3+}(T^{5+}O_4)(T^{5+}O_3OH)(OH)_6$ minerals listed in Table 7.

Acknowledgements

We thank Bill Pinch for initiating this work by providing the crystals as an 'unknown'. This work was supported by a Canada Research Chair in Crystallography and Mineralogy, Research Tools and Equipment, and Discovery Grants from the Natural Sciences and Engineering Research Council of Canada, and Canada Foundation for Innovation Grants, both to FCH.

References

Bayliss, P., Kolitsch, U., Nickel, E.H. and Pring, A. (2010) Alunite supergroup: recommended nomenclature. *Mineralogical Magazine*, **74**, 919–927.

Blount, A.M. (1974) The crystal structure of crandallite. *American Mineralogist*, **59**, 41–47.

Brown, I.D. (2002) The Chemical Bond in Inorganic Chemistry: The Bond Valence Model. Oxford University Press, Oxford, UK.

Brown, I.D. and Altermatt, D. (1985) Bond-valence parameters obtained from a systematic analysis of the inorganic crystal structure database. *Acta Crystallographica*, **B41**, 244–247.

Bruker (1997) *SHELXTL Reference Manual 5.1*. Bruker AXS Inc., Madison, Wisconsin, USA.

Dzikowski, T.J., Groat, L.A. and Jambor, J.L. (2006) The symmetry and crystal structure of gorceixite, $BaAl_3[PO_3(O,OH)]_2(OH)_6$, a member of the alunite supergroup. *The Canadian Mineralogist*, **44**, 951–958.

Gebhard, G. (1999) *Tsumeb II. A Unique Mineral Locality*. GG Publishing, Grossenseifen, Germany.

Giuseppetti, G. and Tadini, C. (1980) The crystal structure of osarizawaite. *Neues Jahrbuch für Mineralogie Monatshefte*, **1980**, 401–407.

Giuseppetti, G. and Tadini, C. (1987) Corkite, $PbFe_3(SO_4)(PO_4)(OH)_6$, its crystal structure and ordered arrangement of the tetrahedral cations. *Neues Jahrbuch für Mineralogie, Monatshefte*, **1987**, 71–81.

Grey, I.E., Mumme, W.G., Mills, S.J., Birch, W.D. and Wilson, N.C. (2009) The crystal chemical role of Zn in alunite-type minerals: structure refinements for kintoreite and zincian kintoreite. *American Mineralogist*, **94**, 676–683.

Hawthorne, F.C., Ungaretti, L. and Oberti, R. (1995) Site populations in minerals: terminology and presentation of results of crystal-structure refinement. *The Canadian Mineralogist*, **33**, 907–911.

Kato, T. (1987) Further refinement of the goyazite structure. *Mineralogical Journal*, **13**, 390–396.

Kolitsch, U. and Pring, A. (2001) Crystal chemistry of the crandallite, beudantite and alunite groups: a review and evaluation of the suitability as storage materials for toxic metals. *Journal of Mineralogical and Petrological Sciences*, **96**, 67–78.

Kolitsch, U., Slade, P.G., Tiekink, E.R.T. and Pring, A. (1999*a*) The structure of antimonian dussertite and the role of antimony in oxysalt minerals. *Mineralogical Magazine*, **63**, 17–26.

Kolitsch, U., Taylor, M.R., Fallon, G.D. and Pring, A.

(1999*b*) Springcreekite, $BaV_3^{3+}(PO_4)_2(OH,H_2O)_6$, a new member of the crandallite group, from the Spring Creek mine, South Australia: the first natural V^{3+}-member of the alunite family and its crystal structure. *Neues Jahrbuch für Mineralogie, Monatshefte*, **1999**, 529–544.

Kolitsch, U., Tiekink, E.R.T., Slade, P.G., Taylor, M.R. and Pring. A. (1999*c*) Hinsdalite and plumbogummite, their atomic arrangements and disordered lead sites. *European Journal of Mineralogy*, **11**, 513–520.

Mills, S.J., Kampf, A.R., Raudsepp, M. and Christy, A.G. (2009) The crystal structure of Ga-rich plumbogummite from Tsumeb, Namibia. *Mineralogical Magazine*, **73**, 837–845.

Pinch. W.W. and Wilson, W.E. (1977) Tsumeb V. Minerals: A descriptive list. *Mineralogical Record*, **8**(3), 17–37.

Pouchou, J.L. and Pichoir, F. (1985) 'PAP' φ(ρZ) procedure for improved quantitative microanalysis. Pp. 104–106 in: *Microbeam Analysis* (J.T. Armstrong, editor). San Francisco Press, San Francisco, California, USA.

Sato, E., Nakai, I., Miyawaki, R. and Matsubara, S. (2009) Crystal structures of alunite family minerals: beaverite, corkite, alunite, natroalunite, jarosite, svanbergite, and woodhouseite. *Neues Jahrbuch für Mineralogie, Abhandlungen*, **183**, 313–322

Schmetzer, K., Tremmel, G. and Medenbach, O. (1982) Philipsbornit, $PbAl_3H[(AsO_4)_2]$, aus Tsumeb, Namibia – ein zweites Vorkommen. *Neues Jahrbuch für Mineralogie, Monatshefte*, **1982**, 248–254.

Sheldrick, G.M. (2008) A short history of *SHELX*. *Acta Crystallographica*, **A64**, 112–122.

Smith, R.L., Simons, F.S. and Vlisidis, A.C. (1953) Hidalgoite, a new mineral. *American Mineralogist*, **38**, 1218–1224.

Szymanski, J.T. (1985) The crystal structure of plumbojarosite, $Pb[Fe_3(SO_4)_2(OH)_6]_2$. *The Canadian Mineralogist*, **23**, 659–668.

Walenta, K., Zwiener, M. and Dunn, P.J. (1982) Philipsbornit, ein neues Mineral der Crandallitreihe von Dundas auf Tasmania. *Neues Jahrbuch für Mineralogie, Monatshefte*, **1982**, 1–5.

Weber, D. and Wilson, W.E. (1977) Tsumeb IV. Geology. *Mineralogical Record*, **8**(3), 14–16.